# Journal of Applied Sciences

ISSN 1812-5654

science alert

ANSInet
an open access publisher
http://ansinet.com

Journal of Applied Sciences 8 (2): 262-270, 2008
ISSN 1812-5654
© 2008 Asian Network for Scientific Information

# Computation of Surface Roughness of Mountains Extracted from Digital Elevation Models

S. Dinesh
Science and Technology Research Institute for Defence (STRIDE),
Ministry of Defence, Malaysia

**Abstract:** In this study, a procedure to compute the surface roughness of individual mountain objects extracted from Digital Elevation Models (DEMs) is proposed. First, mathematical morphology is employed to extract the mountains of the DEM. The lifting scheme is employed to perform the generation of multiscale DEMs. The mask of pixels modified in each mountain object at each scale is computed by performing the intersection operation between the mountain object and the mask of pixels modified at each scale. The normalized probability functions for each mountain object are computed as the ratio of the area of pixels modified in the mountain object at each scale to the area of the mountain object. The computed normalized probability functions are used to compute the scale-independent average roughness of the mountain objects due to the distribution of convex and concave regions averaged over the mountain objects. The proposed methodology allows for a more accurate quantification of a region's convexity/concavity over varying scales, distinguishing between shallow and deep incisions and hence provides a more accurate surface roughness parameter. It is observed that the larger the area of the mountain object, the higher is its surface roughness.

**Key words:** Mountains, multiscale digital elevation models, lifting scheme, convex and concave regions, normalized distribution function, surface roughness

## INTRODUCTION

In the past few decades, the quantitative computation of surface roughness has received increasing attention due to its importance in numerical surface study. A number of algorithms have been employed to compute surface roughness; a summary can be found in Shepard *et al.* (2001) and Li *et al.* (2005). The most commonly used roughness parameter and the easiest to obtain, is the Root-Mean-Square (RMS) height, or the standard deviation of heights above the mean (Brock, 1983). The profile is first detrended by subtracting a best fit linear function from the data, leaving a series of heights with a mean value of zero. This approach is insensitive to amplitude differences and is not a good frequency discriminator. An alternative approach is to fit a plane to a surface and use the error as an estimate of the surface roughness (Wilcox and Gennery, 1987). In the case of two sinusoidal surfaces of differing frequencies, plane fitting suffers from a fundamental shortcoming by producing the same roughness estimation. Stone and Dugundji (1965) propose a method of computing surface roughness using Fourier analysis. This method measures roughness along specific directions of a surface and includes amplitude, frequency and autocorrelation terms. This approach provides surface roughness parameters that have consistent representation in the frequency domain. However, as it depends on the direction of measurement, it is influenced by the rotation and translation of the surface. The slope and intercept of the logarithmic plot of the power spectrum of the terrain profile is reported as a roughness parameter by van Zyl *et al.* (1991). However, there is no simple correspondence between the intercept or the slope of the logarithmic plot of the power spectrum and commonly used roughness measures. Other reported roughness measures, developed to overcome these shortfalls, include effective slope (Miller and Parsons, 1990; Campbell and Garvin, 1993), autocorrelation length (Turcotte, 1997), radiosity models (Li *et al.*, 1998), median and absolute slope (Kreslavsky and Head, 1999), granulometry (Tay *et al.*, 2005a) and high-order statistics (Nikora, 2005). These algorithms, which operate at singular scales of measurement, provide scale-dependant roughness parameters.

Dinesh (2007a) proposes a procedure to compute a scale-independent surface roughness parameter from Digital Elevation Models (DEMs). First, multiscale DEMs are generated using the lifting scheme. The area of pixels modified at each scale is computed. The computed areas are divided with the area of the DEM to obtain the normalized probability functions, which are used to

compute the average size of convex and concave regions in the DEM and the scale-independent average roughness of the terrain of the DEM due to the distribution of convex and concave regions in the terrain.

In this study, the procedure proposed in Dinesh (2007a) is extended to perform the computation of surface roughness of individual mountain objects extracted from DEMs.

## MATERIALS AND METHODS

**The Global Digital Elevation Model (GTOPO30) of Great Basin:** The DEM in Fig. 1 shows the area of Great Basin, Nevada, USA. The area is bounded by latitude 38° 15' to 42° N and longitude 118° 30' to 115° 30' W. The DEM was rectified and resampled to 925 m in both x and y directions. The DEM is a Global Digital Elevation Model (GTOPO30) and was downloaded from the USGS GTOPO30 website (http://edcwww.cr.usgs.gov/landdaac/gtopo30/gtopo30.html). GTOPO30 DEMs are available at a global scale, providing a digital representation of the Earth's surface at a 30 arc-seconds sampling interval. The land data used to derive GTOPO30 DEMs are obtained from Digital Terrain Elevation Data (DTED), the 1-degree DEM for USA and the Digital Chart of the World (DCW). The accuracy of GTOPO30 DEMs varies by location according to the source data. The DTED and the 1-degree dataset have a vertical accuracy of ±30 m while the absolute accuracy of the DCW vector dataset is ±2000 m horizontal error and ±650 m vertical error (Miliaresis and Argialas, 2002).

**Mountain extraction:** Mountains are the portions a terrain that are sufficiently elevated above the surrounding land (greater than 300 to 600 m) and have comparatively steep sides. In a mountain, two parts are distinctive:

- The summit, the highest point (the peak) or the highest ridges.
- The mountainside, the part of a mountain between the summit and the foot (Bates and Jackson, 1987).

The mapping of mountains is generally performed manually through fieldwork and visual interpretation of topographic maps, which is a time consuming and labor intensive activity. In recent times, extraction techniques have evolved from manual through computer assisted to automated methods with DEMs as the input data. In seeking the efficient extraction of mountains from DEMs, various algorithms have been proposed (Graff and Usery, 1993; Miliaresis and Argialas, 1999; Miliaresis, 2000; Dinesh, 2006).

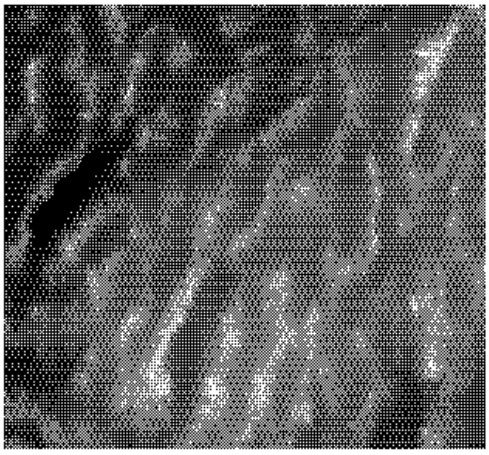

Fig. 1: The GTOPO30 DEM of Great Basin. The elevation values of the terrain (minimum 1005 m and maximum 3651 m) are rescaled to the interval of 0 to 255 (the brightest pixel has the highest elevation). The scale is approximately 1:3,900,00

The mountains of the DEM of Great Basin are extracted using the mathematical morphological based algorithm proposed in Dinesh (2006). First, ultimate erosion is performed on the DEM to extract the peaks of the DEM. Conditional dilation is performed on the extracted peaks to obtain the mountains of the DEM. A total of 14 distinct individual mountains objects are extracted from the DEM (Fig. 2).

**Generation of multiscale DEMS using the lifting scheme:** Feature detection and characterization often need to be performed at different of scales measurement. Wood (1996a, b) shows that analysis of a location at multiple scales allows for a greater amount of information to be extracted from a DEM about the spatial characteristics of a feature. The term scale refers to combination of both spatial extent and spatial detail or resolution (Goodchild and Quattrochi, 1997; Tate and Wood, 2001). A number of research efforts have been conducted to characterize geomorphological features, such as drainage and ridge networks (Radhakrishnan, 2002, 2003, 2004; Sagar *et al*., 2003; Tay *et al*., 2005b), catchments (Dinesh, 2007b) and mountains (Dinesh, 2007c,d,e; Dinesh and Fadzil, 2007a,b), using the variation in the spatial extent over which these features are defined.

In this study, multiscaling is performed using the lifting scheme (Sweldens, 1996, 1997). The lifting scheme is a flexible technique that has been used in several different settings, for easy construction and

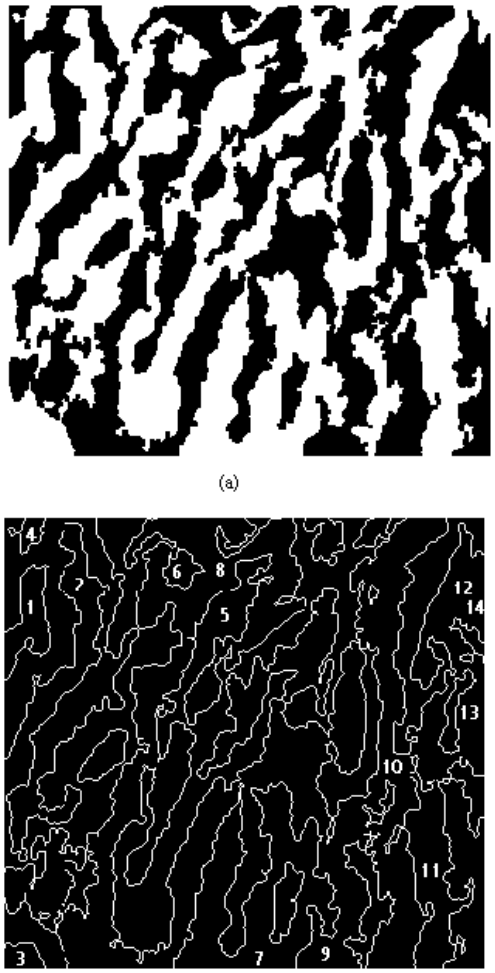


(a)

(b)

Fig. 2: Extraction of mountains from DEM. (a) The extracted mountains and (b) A total of 14 individual mountains objects are identified using connected component labeling (Pitas, 1993)

implementation of traditional wavelets and of second generation wavelets, such as spherical wavelets. Lifting consists of the following three basic operations:

**Step 1: Split:** The original data set x[n] is divided into two disjoint subsets, even indexed points $x_e[n] = x[2n]$ and odd indexed points $x_0[n] = x[2n+1]$.

**Step 2: Predict:** The odd and even subsets are often highly correlated. This correlation structure typically local and hence, it is possible to accurately predict the wavelet coefficients d[n] as the error in predicting $x_0[n]$ from $x_e[n]$ using the prediction operator P:

$$d[n] = x_o[n] - p(x_e[n]) \quad (1)$$

Where:

$$P(x_e[n]) = \frac{1}{2}(x_e[n] + x_e[n+1]) \quad (2)$$

**Step 3: Update:** Scaling coefficients c[n] that represent a coarse approximation to the signal x[n] are obtained by combining $x_e[n]$ and d[n]. This is accomplished by applying an update operator U to the wavelet coefficients and adding to $x_e[n]$:

$$c[n] = x_e[n] + U(d[n]) \quad (3)$$

Where:

$$U(d[n]) = \frac{1}{4}(d[n-1] + d[n+1]) \quad (4)$$

These three steps form a lifting stage. The lifting scheme scans 2D images row-by-row. Using a DEM as the input, an iteration of the lifting stage generates the complete set of multiscale DEMs $c_r[n]$ and the elevation loss caused by the change of scale $d_r[n]$.

Multiscale DEMs of the Great Basin region are generated by implementing the lifting scheme on the DEM of Great Basin using scales of 1 to 20. As shown in Fig. 3, as the scale increases, the merge of small regions into the surrounding grey level regions increases, causing removal of fine detail in the DEM. The fine detail in DEMs represents crenulations, which are used to extract hydrological features from DEMs. Convex crenulations are used to extract ridge networks while concave crenulations are used to extract drainage networks (Gilbert, 1909; Howard, 1994; Rodríguez-Iturbe and Rinaldo, 1997). The distribution of convex and concave regions in a terrain indicates the surface roughness of the terrain. The removal of convex and concave regions from the terrain during the multiscaling process results in the terrain becoming smoother.

The mask of pixels modified at each scale r is identified by computing the difference between the DEM of scale r and the DEM of the previous scale r-1. The resulting image is thresholded into a binary image by converting all pixels with grey level more than 0 to binary 1 and all pixels with grey level 0 to binary 0. The computed masks of pixels modified are shown in Fig. 4.

**Computation of surface roughness of individual mountain objects:** The procedure proposed to perform the computation of surface roughness of the individual mountain objects is demonstrated using the first mountain object (Fig. 5). The mask of pixels modified in the each

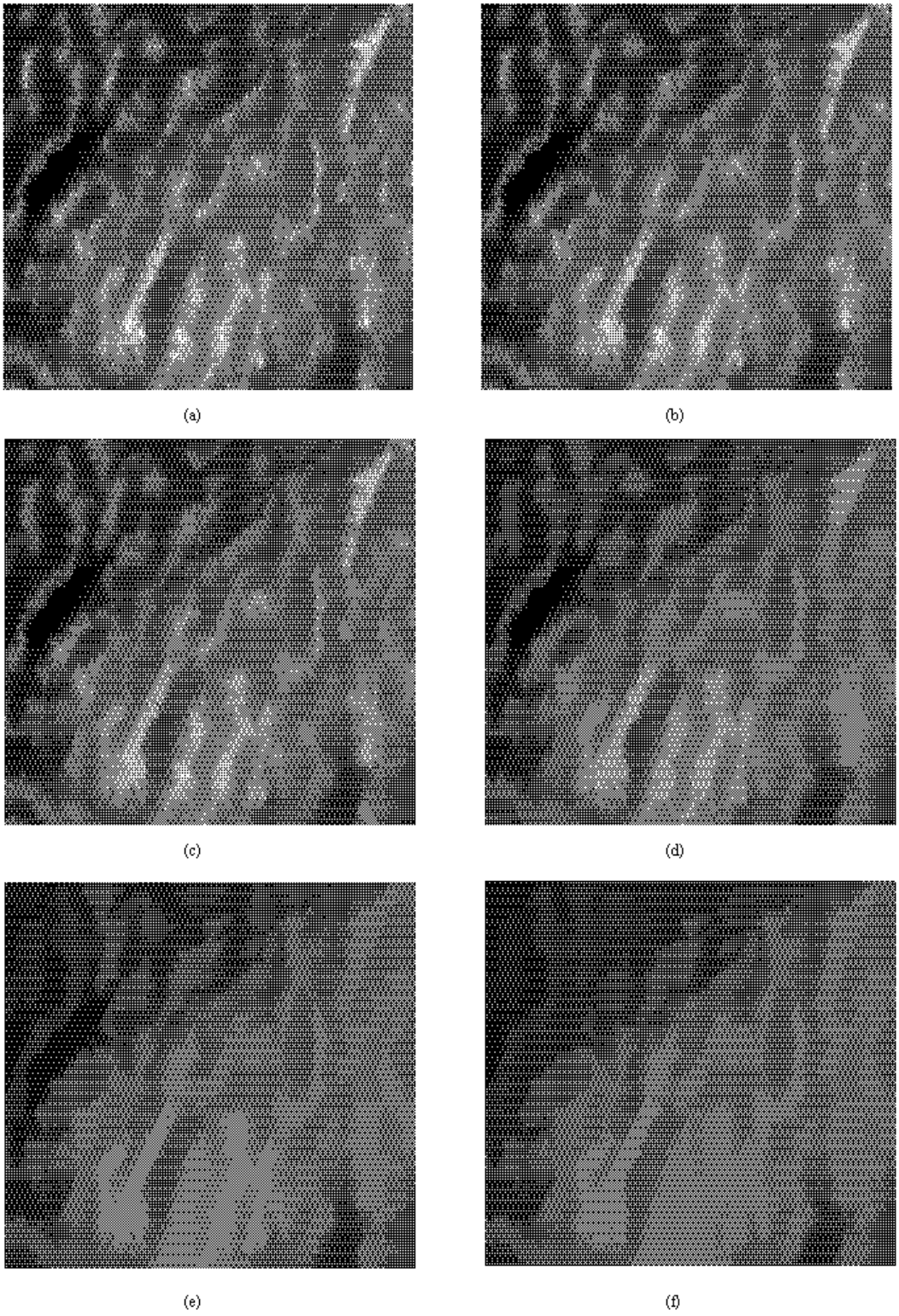


Fig. 3: Multiscale DEMs generated using scales of (a) 1 (b) 3 (c) 5 (d) 10 (e) 15 and (f) 20

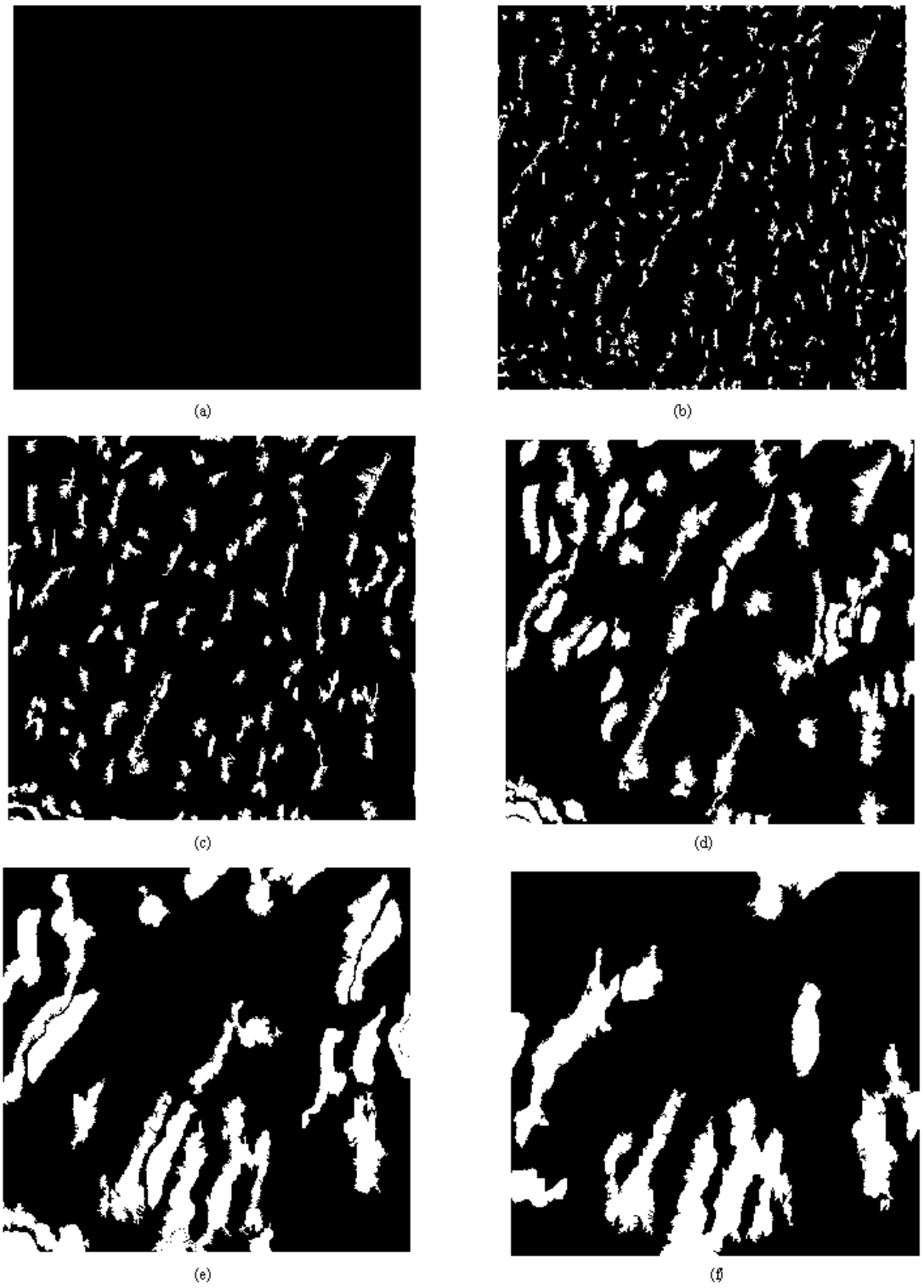


Fig. 4: Mask of pixels modified during the multiscaling process for the corresponding multiscale DEMs in Fig. 3. This indicates the convex and convex regions removed from the DEM during the multiscaling process

Fig. 5: The first mountain object

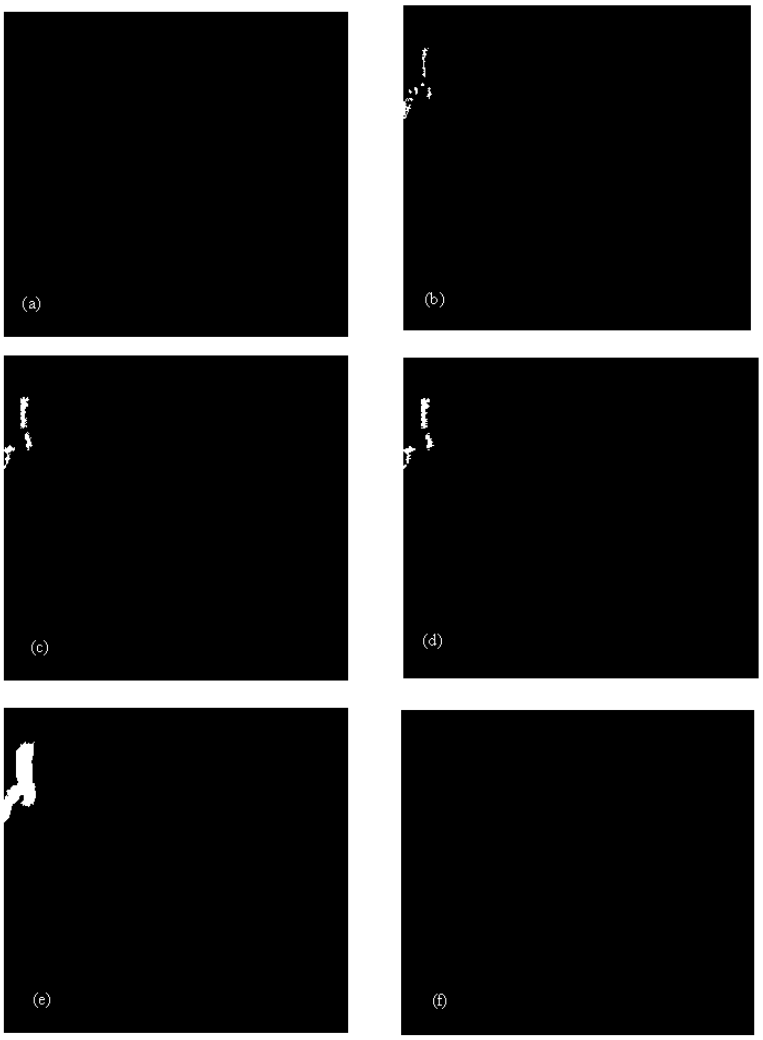


Fig. 6: The mask of pixels modified in the first mountain object during the multiscaling process for the corresponding multiscale DEMs in Fig. 3. This indicates the convex and convex regions removed from the mountain object during the multiscaling process

Table 1: The computed values of $S_0$ and H for the individual mountain objects

| Mountain object ID | Area $S_0$ (pixels) | Average roughness H |
|---|---|---|
| 1 | 1227 | 1.80 |
| 2 | 10422 | 2.65 |
| 3 | 1353 | 2.28 |
| 4 | 298 | 1.39 |
| 5 | 14232 | 2.62 |
| 6 | 432 | 2.02 |
| 7 | 6444 | 2.28 |
| 8 | 311 | 2.09 |
| 9 | 1119 | 1.71 |
| 10 | 219 | 0.88 |
| 11 | 3574 | 2.58 |
| 12 | 3058 | 2.25 |
| 13 | 494 | 1.54 |
| 14 | 261 | 1.80 |

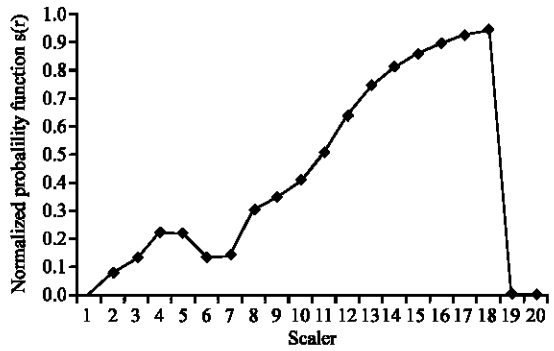


Fig. 7: Plot of the normalized probability functions of the first mountain object s(r) against the scale r

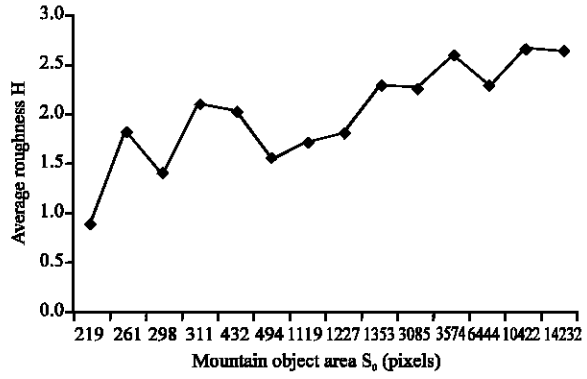


Fig. 8: Plot of the area of the mountains object $S_0$ against the average roughness of the mountains object H

mountain object at each scale (Fig. 6) is computed by performing the intersection operation between the mountain object and the mask of pixels modified at each scale. The normalized probability functions of the mountain object s(r) are computed as the ratio of the area of pixels modified in the mountain object at each scale S(r) to the area of the mountain object $S_0$.

$$s(r) = S(r)/S_0 \quad (5)$$

A larger value of s(r) indicates a larger area of convex and concave regions removed at scale r. As observed in Fig. 7, s(r) increases as the scale is increased, indicating the importance of multiscale analysis in surface roughness computation. At scales 19 and above, s(r) has a value of 0, indicating that all convex and concave regions in the mountain object have been removed.

The computed values of s(r) are used to compute average roughness of the extracted mountains H, which indicates surface roughness of the mountain object due to the convex and concave region distribution averaged over the area of the mountain object. H is computed using the following equation, which is due to Maragos (1989):

$$H = \sum_{r=1}^{20} s(r) \log s(r) \quad (6)$$

H for the first mountain object is computed to be 1.79. The proposed procedure is employed to compute the values of H for the remaining mountains objects (Table 1). The proposed methodology allows for a more accurate quantification of a region's convexity/concavity over varying scales, distinguishing between shallow and deep incisions and hence provides a more accurate surface roughness parameter. It is observed in Fig. 8 that the larger the area of the mountain object, the higher is its surface roughness. This observation is consistent with the findings reported in Miliaresis and Argialas (2002).

## CONCLUSION

In this study, a procedure to compute the surface roughness of individual mountain objects extracted from Digital Elevation Models (DEMs) was proposed. First, mathematical morphology was employed to extract the mountains of the DEM. The lifting scheme was employed to perform the generation of multiscale DEMs. The mask of pixels modified in the each mountain object at each scale was computed by performing the intersection operation between the mountain object and the mask of pixels modified at each scale. The normalized probability functions for each mountain object were computed as the ratio of the area of pixels modified in the mountain object at each scale to the area of the mountain object. The computed normalized probability functions were used to compute the average size of convex and concave regions in the mountain objects and the scale-independent average roughness of the mountain objects due to the convex and concave region distribution averaged over the mountain objects. The proposed methodology allows for

a more accurate quantification of a region's convexity/concavity over varying scales, distinguishing between shallow and deep incisions and hence provides a more accurate surface roughness parameter. It was observed that the larger the area of the mountain object, the higher is its surface roughness.

## ACKNOWLEDGMENTS

The author is grateful to four anonymous reviewers for their comments that have helped strengthen this study.

## REFERENCES

Bates, R.L. and J.A. Jackson, 1987. Glossary of Geology. Alexandria, American Geological Institute, Virginia.

Brock, M., 1983. Surface roughness analysis. Brüel and Kjær Instruments Inc., Nærum, Denmark.

Campbell, B.A. and J.B. Garvin, 1993. Lava flow topographic measurements for radar data interpretation. Geophy. Res. Lett., 20 (9): 831-834.

Dinesh, S., 2006. Extraction of mountains from digital elevation models using mathematical morphology. GIS Dev. Malaysia, 1 (4): 16-19.

Dinesh, S., 2007a. Characterization of areas of pixels modified during the generation of multiscale digital elevation models. J. Applied Sci. (In Press).

Dinesh, S., 2007b. Characterization of catchments extracted from multiscale digital elevation models. Applied Math. Sci., 1 (20): 963-974.

Dinesh, S., 2007c. Fuzzy classification of physiographic features extracted from multiscale digital elevation models. Applied Math. Sci., 1 (19): 939-961.

Dinesh, S., 2007d. Fuzzy classification of mountains extracted from multiscale digital elevation models. Regional Annual Fundamental Science Seminar 2007 (RAFSS 2007), 28th-29th May 2007, Ibnu Sina Institute for Fundamental Science Studies, Universiti Teknologi Malaysia, Malaysia.

Dinesh, S., 2007e. Computation of the number and area frequency dimensions of mountains extracted from multiscale digital elevation models. Applied Math. Sci., 1 (40): 1969-1989.

Dinesh, S. and M.H.A. Fadzil, 2007a. Characterization of the size distribution of mountains extracted from multiscale digital elevation models. J. Applied Sci., 7 (10): 1410-1415.

Dinesh, S. and M.H.A. Fadzil, 2007b. Characterization of the size distribution of mountains extracted from digital elevation models: A multiscale approach. 4th Biannual Postgraduate Research Symposium, 5th-9th February 2007, Universiti Teknologi Petronas (UTP), Perak.

Gilbert, G.K., 1909. The convexity of geology. J. Geol., 17: 344-350.

Goodchild, M.F. and D.A. Quattrochi, 1997. Scale, Multiscaling, Remote Sensing and GIS. In: Scale in Remote Sensing and GIS, Quattrochi, D.A. and M.F. Goodchild (Eds.). Lewis Publishers, Boca Raton, Florida, pp: 1-11.

Graff, L.H. and E.L. Usery, 1993. Automated classification of generic terrain features in digital elevation models. Photogrammetric Eng. Remote Sens., 59 (9): 1409-1417.

Howard, A.D., 1994. A detachment-limited model of drainage basin evolution. Water Resour. Res., 30 (7): 2261-2285.

Kreslavsky, M.A. and J.W. Head, 1999. Kilometer-scale slopes on Mars and their correlation with geologic units: Initial results from Mars Orbiter Laser Altimeter (MOLA) data. J. Geophy. Rev., 104 (E9): 21,911-21,924.

Li, W.H., R. Weeks and Gillispie, 1998. Multiple scattering in the remote sensing of natural surfaces. Int. J. Remote Sens., 19 (9): 1725-1740.

Li, Z., Q. Zhu and C. Gold, 2005. Digital Terrain Modelling: Principles and Methodology. CRC Press, New York.

Maragos, P., 1989. Pattern spectrum and multiscale shape representation. IEEE T. Pattern Anal., 11 (7): 701-716.

Miliaresis, G.C. and D.P. Argialas, 1999. Segmentation of physiographic features from Global Digital Elevation Model/GTOPO30. Comput. Geosci., 25 (7): 715-728.

Miliaresis, G.C., 2000. The DEM to mountain transformation of Zagros Ranges. 5th International Conference on GeoComputation, 23-25 of August 2000, University of Greenwich.

Miliaresis, G.C. and D.P. Argialas, 2002. Quantitative representation of mountain objects extracted from the Global Digital Elevation Model (GTOPO30). Int. J. Remote S., 23 (5): 949-964.

Miller, L.S. and C.L. Parsons, 1990. Rough surface scattering results based on bandpass autocorrelation forms. IEEE Geosci. Remote Sens., 28: 1017-1021.

Nikora, V., 2005. High-order structure functions for planet surfaces: A turbulence metaphor. IEEE Geosci. Remote Sens. Lett., 2 (3): 362-365.

Pitas, I., 1993. Digital Image Processing Algorithms. Prentice Hall, London.

Radhakrishnan, P., 2002. Characterization of multi-scale connectivity networks derived from simulated fractal image in discrete space. Asian Technology Conference in Mathematics 2002, 17th-21st December 2002, Multimedia University, Malaysia.

Radhakrishnan, P., 2003. Multi-fractal behavior of connectivity network. Proceedings of International Conference n Robotics, Vision, Information And Signal Processing (IEEE), pp: 202-205.

Radhakrishnan, P., 2004. Discrete simulation, spatial modelling and characterization of certain geophysical phenomena. Ph.D. Thesis, Multimedia University, Malaysia.

Rodríguez-Iturbe, I. and A. Rinaldo, 1997. Fractal River Basins: Chance and Self-Organization. Cambridge University Press, New York.

Sagar, B.S.D., M.B.R. Murthy, C. Rao and B. Raj, 2003. Morphological approach to extract ridge-valley connectivity networks from digital elevation models. Int. J. Remote Sens., 24: 573-581.

Shepard, M.K., B.A. Campbell, M.H. Bulmer, T.G. Farr, L.R. Gaddis and J.J. Plaut, 2001. The roughness of natural terrain: A planetary and remote sensing perspective. J. Geophys. Res., 106 (E12): 777-795.

Stone, R. and J. Dugundji, 1965. A study of microrelief: Its mapping, classification and quantification by means of a Fourier analysis. Eng. Geol., 1 (2): 89-187.

Sweldens, W., 1996. The lifting scheme: A custom-design construction of biothorgonal wavelets. Applied Comput. Harmon. Anal., 3 (2): 186-200.

Sweldens, W., 1997. The lifting scheme: A construction of second generation wavelets. J. Math. Anal., 29 (2): 511-546.

Tate, N. and J. Wood, 2001. Fractals and Scale Dependencies in Topography. In: Modelling Scale in Geographical Information Science, Tate, N. and P. Atkinson (Eds.). Wiley, Chicester, pp: 35-51.

Tay, L.T., B.S.D. Sagar and H.T. Chuah, 2005a. Derivation of terrain roughness indicators via granulometries. Int. J. Remote Sens., 24 (3): 573-581.

Tay, L.T., B.S.D. Sagar and H.T. Chuah, 2005b. Analysis of geophysical networks derived from multiscale digital elevation models: A morphological approach. IEEE Geosci. Remote Sens., 2 (4): 399-403.

Turcotte, D.L., 1997. Fractals and Chaos in Geology and Geophysics. Cambridge University Press, New York.

van Zyl, J.J., C.F. Burnette and T.G. Farr, 1991. Inference of surface power spectra from inversion of multifrequency polarimetric radar data. Geophys. Res. Lett., 18 (9): 1787-1790.

Wilcox, B. and D. Gennery, 1987. A Mars rover for the 1990's. J. Br. Planetary Soc., 40 (10): 484-488.

Wood, J., 1996a. Scale-Based Characterization of Digital Elevation Models. In: Innovation in GIS 3, Parker, D. (Eds.). Taylor and Francis, London, pp: 163-175.

Wood, J., 1996b. The geomorphological characterization of digital elevation models. Ph.D. Thesis, University of Leicester, Leicester.